Two mechanistically distinct effects of dihydropyridine nifedipine on $Ca_V1.2$ L-type Ca^{2+} channels revealed by Timothy syndrome mutation

Xiaona Sheng [a, b, c], Tsutomu Nakada [a], Motohiro Kobayashi [d], Toshihide Kashihara [a], Toshihide Shibazaki [a, e], Miwa Horiuchi-Hirose [a], Simmon Gomi [a, f], Masamichi Hirose [g], Toshifumi Aoyama [b], Mitsuhiko Yamada [a,*]

[a] Department of Molecular Pharmacology, Shinshu University School of Medicine, Matsumoto, Nagano, Japan; [b] Department of Metabolic Regulation, Institute on Aging and Adaptation, Shinshu University Graduate School of Medicine, Matsumoto, Nagano, Japan; [c] Department of Neurology, The Second Hospital of Hebei Medical University, Shijiazhuang, Hebei, China; [d] Department of Molecular Pathology, Shinshu University Graduate School of Medicine, Matsumoto, Nagano, Japan; [e] Discovery Research Laboratory II, R&D, Kissei Pharmaceutical Co., Ltd., Azumino, Nagano Japan; [f] Department of Cardiovascular Medicine, Shinshu University School of Medicine, Matsumoto, Nagano, Japan; and [g] Department of Molecular and Cellular Pharmacology, School of Pharmaceutical Sciences Iwate Medical University, Morioka, Iwate, Japan

*Corresponding author: Mitsuhiko Yamada, MD PhD,
Department of Molecular Pharmacology, Shinshu University School of Medicine
3-1-1 Asahi, Matsumoto, Nagano 390-8621 Japan. Tel: +81-263-37-2605; Fax: +81-263-37-2605;
Email: myamada@shinshu-u.ac.jp

Abstract

Dihydropyridine Ca^{2+} channel antagonists (DHPs) block $Ca_V1.2$ L-type Ca^{2+} channels (LTCCs) by stabilizing their voltage-dependent inactivation (VDI); however, it is still not clear how DHPs allosterically interact with the kinetically distinct (fast and slow) VDI. Thus, we analyzed the effect of a prototypical DHP, nifedipine on LTCCs with or without the Timothy syndrome mutation that resides in the I-II linker (L_{I-II}) of $Ca_V1.2$ subunits and impairs VDI. Whole-cell Ba^{2+} currents mediated by rabbit $Ca_V1.2$ with or without the Timothy mutation (G436R) (analogous to the human G406R mutation) were analyzed in the presence and absence of nifedipine. In the absence of nifedipine, the mutation significantly impaired fast closed- and open-state VDI (CSI and OSI) at -40 and 0 mV, respectively, but did not affect channels' kinetics at -100 mV. Nifedipine equipotently blocked these channels at -80 mV. In wild-type LTCCs, nifedipine promoted fast CSI and OSI at -40 and 0 mV and promoted or stabilized slow CSI at -40 and -100 mV, respectively. In LTCCs with the mutation, nifedipine resumed the impaired fast CSI and OSI at -40 and 0 mV, respectively, and had the same effect on slow CSI as in wild-type LTCCs. Therefore, nifedipine has two mechanistically distinct effects on LTCCs: the promotion of fast CSI/OSI caused by L_{I-II} at potentials positive to the sub-threshold potential and the promotion or stabilization of slow CSI caused by different mechanisms at potentials negative to the sub-threshold potential.

Keywords

$Ca_V1.2$ L-type Ca^{2+} channel

Voltage-dependent inactivation

Dihydropyridine

Nifedipine

Timothy syndrome

Allosteric model

1. Introduction

L-type Ca^{2+} channels (LTCCs) mediate Ca^{2+} influx into cells in response to membrane depolarization (Catterall, 2000). The amino acid sequence of their main Ca_V1 subunits is organized into four repeated domains (I-IV), each of which contains six transmembrane segments (S1-S6). Upon membrane depolarization, LTCCs open and are then inactivated. The inactivation of LTCCs is driven by intracellular Ca^{2+} and the membrane potential (VDI) (Hering et al., 2000; Soldatov, 2003; Stotz et al., 2004; Zuhlke et al., 1999). VDI occurs regardless whether channels are open (open-state inactivation (OSI)) or closed (closed-state inactivation (CSI)). Both CSI and OSI of LTCCs occur in a biexponential time course, indicating that LTCCs have at least two kinetically distinct (fast and slow) VDI states. The intracellular linker between the I and II domains of Ca_V subunits (L_{I-II}) participates in the fast OSI of neuronal P/Q and R-types of Ca^{2+} channels (Herlitze et al., 1997; Stotz et al., 2000; Stotz et al., 2004). On the other hand, the mechanism of slow OSI probably includes a more global conformational change of Ca_V subunits (Hering et al., 2000; Kobrinsky et al., 2004; Shi and Soldatov, 2002; Soldatov, 2003) and the immobilization of a gating charge (Hadley and Lederer, 1991; Shirokov et al., 1992).

LTCCs are selectively inhibited by dihydropyridine (DHP) antagonists (Hockerman et al., 1997), which block LTCCs by binding to IIIS5, IIIS6 and IVS6 of Ca_V1 subunits and stabilize the nonconducting state of LTCCs with a single Ca^{2+} ion in the selectivity filter (Peterson and Catterall, 2006). DHP antagonists bind to LTCCs with the highest affinity for the inactivated state (Bean, 1984; Lee and Tsien, 1983; Sanguinetti and Kass, 1984). DHP antagonists cause a tonic block and gating charge immobilization of LTCCs at potentials negative to the threshold potential for channel opening (Bean, 1984; Hadley and Lederer, 1991; Lee and Tsien, 1983; Sanguinetti and Kass, 1984). Some DHP antagonists also cause a phasic block of LTCCs by accelerating OSI at potentials positive to the threshold potential (Berjukow and Hering, 2001; Berjukow et al., 2000; Handrock et al., 1999; Hess et al., 1984; Lacinova et al., 2000; Lee and Tsien, 1983; Sanguinetti and Kass, 1984): however, it has not been clarified how these distinct effects of DHPs take place in relation to the fast and slow CSI/OSI.

Here, we analyzed the effect of a prototypical DHP antagonist nifedipine on the fast and slow CSI/OSI of recombinant rabbit $Ca_V1.2$ LTCCs with or without the G436R mutation that impairs OSI (Raybaud et al., 2006; Yarotskyy et al., 2009). This mutation corresponds to the G406R mutation that resides at $L_{I\text{-}II}$ in human $Ca_V1.2$ subunits and causes Timothy syndrome, a human disorder associated with fatal ventricular arrhythmias, syndactyly, immune deficiency and autism (Splawski et al., 2004). In this study, we show that nifedipine promotes fast CSI and OSI caused by $L_{I\text{-}II}$ at potentials positive to the sub-threshold potential, and promotes or stabilizes slow CSI at potentials negative to the sub-threshold potential.

2. Materials and Methods

2.1 Molecular Biology

The investigation conformed to the *Guide for the Care and Use of Laboratory Animals* published by the US National Institutes of Health (NIH Publication No. 85-23, revised 1996). This study was approved by the Committee for Animal Experimentation of Shinshu University (approval number: 220024). All experiments described in this study were carried out in accordance with the Guidelines for Animal Experimentation of Shinshu University. Rats were sacrificed by sodium pentobarbital (30 mg/kg) anesthesia administrated intraperitoneally, and the heart and brain were excised from the animals. Total RNA of these tissues was extracted with Isogen (Nippon Gene Co. Ltd., Tokyo, Japan) according to the manufacturer's instructions. Total RNA was reverse transcribed by the SuperScript III First-Strand Synthesis System for reverse transcription-PCR (Invitrogen Inc., Carlsbad, CA). The cDNAs of $\alpha_2\delta_1$ (GenBank ID: NM001110847) and β_{2a} (GenBank ID: NM053851) were amplified by PCR with DNA polymerase PrimeSTAR HS from the heart and brain total cDNA, respectively (Takara Bio Inc., Shiga, Japan). The sequence of primers used was 5'-TGATCTTCGATCGCGAAGATGG-3' ($\alpha_2\delta_1$, sense), 5'-AGGGCATGGAATTAAGTTGCAGA-3' ($\alpha_2\delta_1$, antisense), 5'- AGTGTTGATTTGCCCATGAC-3' (β_{2a}, sense) and 5'-GGCCAATTTCTGTGGTACTT-3' (β_{2a}, antisense). The amplified cDNA fragments encoding $\alpha_2\delta_1$ and β_{2a} were subcloned into pcDNA3.1(-) (Invitrogen) and pcDNA3.1(+)/Hygro (Invitrogen), respectively. The cDNA encoding rabbit $Ca_V1.2$ subunits (GenBank ID: X15539) was generously provided by Prof. William Catterall (University of Washington). The cDNA of $Ca_V1.2$ containing the G436R mutation was generated by the mega-primer method (Kammann et al., 1989). Briefly, the 1st PCR was performed with a primer pair (5'-GAAGATGATCCTTCCCCTTGTGCTC-3' and 5'-TCTTTGGAAAACTCTCTGCTCAACACACCG-3') and wild-type $Ca_V1.2$ cDNA as a template. The 2nd PCR was performed with the 1st PCR product (mega-primer) and an antisense primer (5'-AAGGATTGACCAGTCCCTTGTCAGGTAGTC-3'). Then, a region of wild-type $Ca_V1.2$ cDNA between *Bam*HI and *Afl*II sites was substituted with the PCR product containing the G436R mutation. The nucleotide sequences of all of the constructs were verified with ABI 3130 (Applied

Biosystems, Inc., Foster City, CA).

2.2 Cell Culture

HEK293 cells (ATCC, Manassas, VA) were maintained in Dulbecco's Modified Eagle's Medium (DMEM) (Invitrogen) containing GlutaMAX (Invitrogen), 10% fetal bovine serum (FBS), 100 U/ml penicillin and 100 μg/ml streptomycin. HEK293 cells were transfected with pcDNA3.1(-) harboring the $\alpha_2\delta$□ cDNA with TransFectin Lipid Reagent (Bio-Rad Laboratories, Inc., Richmond, CA) and selected with 800 μg/ml G418. Among several G418-resistant clones, one clone was chosen based on the expression level of $\alpha_2\delta$□ protein as assessed by Western blotting. The selected line was further transfected with pcDNA3.1(+)/Hygro harboring the β_{2a} cDNA and selected with 200 μg/ml hygromycin. Among several hygromycin-resistant clones, one clone was chosen based on the expression level of $\alpha_2\delta$□ and β_{2a} subunits as assessed by Western blotting (Supplementary Fig. 1). For electrophysiological analysis, cDNAs encoding $Ca_V1.2$ (WT) or $Ca_V1.2$ (G436R) (2 μg) and that of EGFP (0.4 μg) were transiently cotransfected into this stable cell line in 2 ml DMEM with TransFectin Lipid Reagent. The expressed LTCC currents were measured 24-72 h after transfection.

2.3 Electrophysiology

The current of LTCCs expressed in HEK293 cells was studied in the whole-cell configuration of the patch clamp technique at 35-37°C with a patch-clamp amplifier (Axopatch 200B; Molecular Devices Corp., Sunnyvale, CA, or EPC 8; HEKA Instruments Inc., Bellmore, NY). Patch pipettes were fabricated from borosilicate glass capillaries (Kimax-51; Kimble Glass Inc., Vineland, NJ). Capacitative currents were eliminated, and the series resistance was compensated by 75% with the patch-clamp amplifiers. The mean series resistance and cell membrane capacitance were 6.26 ± 0.31 MΩ and 39.80 ± 5.12 pF, respectively. The mean voltage error caused by series resistance was 1.74 ± 0.23 mV at 0 mV. To measure LTCC currents, a gigaohm seal was formed with EGFP-positive cells >80% of which expressed LTCC currents. The external solution was modified Tyrode solution containing (in mmol/L): NaCl, 136.5; KCl, 5.4, $CaCl_2$, 1.8; $MgCl_2$, 0.53; HEPES, 5.5; and glucose,

5.5 (pH = 7.4 with NaOH). The pipette solution contained (in mmol/L): D-glutamate, 90; N-methyl-D(-)-glucamine (NMDG), 10; $MgCl_2$, 5; tetraethylammonium chloride, 20, EGTA, 10; HEPES, 20; and MgATP 3 (pH = 7.3 with CsOH). After the whole-cell configuration had been established, triple pulses to -100, -40 and +10 mV (300 ms duration for each pulse) were continuously applied to the cells from the holding potential of -80 mV every 3 s. Then, the bathing solution was switched to external solution 1 containing (in mmol/L): NMDG, 150, CsCl, 5.4; $BaCl_2$, 10; $MgCl_2$, 1.2; 4-aminopyridine, 2; and HEPES, 5 (pH = 7.4 with HCl). About 1 min after currents other than LTCC currents had been suppressed and the amplitude and kinetics of LTCC currents were stable, the membrane potential was held at -80 mV for at least 1 min. The mean peak current amplitude of LTCC channels with or without the G436R mutation (LTCC (G436R) and LTCC (WT)) at 0 mV was -1.55 ± 0.28 and -0.88 ± 0.29 nA, respectively.

To assess the current-voltage relationship of LTCCs, the membrane potential was stepped from -80 mV to potentials between -60 and +60 mV for 500 ms with a 10 mV increment every 60 s. LTCC currents were isolated as the current inhibited by Cd^{2+} (100 μmol/L) plus nifedipine (10 μmol/L) (Yamada et al., 2008). Nifedipine was dissolved at 10 mM in DMSO. The final ≤0.1% DMSO did not affect LTCC currents. The peak density of LTCC currents evoked by the test pulse was plotted against the membrane potential and fit with the following equation:

$$D_{\_peak} = G_{max} \, (1 / (1 + exp \, ((E_{0.5\_Act} - E_m) / k_{\_Act}))) \, (E_m - E_{rev}) \qquad \text{(Eq. 1)}$$

, where $D_{\_peak}$ is the peak current density; G_{max}, maximum conductance density; $E_{0.5\_Act}$, half-maximum activation potential; E_m, membrane potential; $k_{\_Act}$, slope factor of activation; and E_{rev}, apparent reversal potential of LTCC currents.

To assess the concentration-dependent effect of nifedipine, the membrane potential was depolarized from the holding potential of -80 mV to 0 mV for 50 ms every 60 s, and nifedipine dissolved in external solution 1 was applied to cells. The peak LTCC current amplitude in the presence of nifedipine was normalized to that in the presence of 0.1% DMSO, plotted against the

concentration of nifedipine and fit with the following equation:

$$I = 1 / (1 + ([NIF] / K_{0.5})^n) \quad \text{(Eq. 2)}$$

, where I is normalized peak LTCC current amplitude at 0 mV; *[NIF]*, concentration of nifedipine; $K_{0.5}$, the half-maximum inhibitory concentration of nifedipine; and n, Hill coefficient.

To analyze the CSI of LTCCs, the membrane potential was depolarized from -80 mV to 0 mV for 20 ms (P1), repolarized to -80 mV for 5 ms, depolarized to -40 mV for varying durations, repolarized to -80 mV for 5 ms and then depolarized to 0 mV for 20 ms (P2) every 120 s. The peak LTCC current amplitude in P2 was normalized to that in P1, plotted against the duration at -40 mV and fit with the following equation:

$$I = A_0 + A_f \, exp \, (-t / \tau_f) + A_s \, exp \, (-t / \tau_s) \quad \text{(Eq. 3)}$$

, where I is normalized LTCC current amplitude; A_0, amplitude of a non-inactivating component; A_f, amplitude of a fast component; t, time after depolarization to -40 mV; τ_f, time constant of a fast component; A_s, amplitude of a slow component; and τ_s, time constant of a slow component.

To analyze the OSI of LTCCs, the membrane potential was depolarized from -80 mV to 0 mV for 20 s every 120 s. The decay of LTCC currents at 0 mV was fit with Eq. 3.

To assess the recovery from inactivation, the membrane potential was stepped from the holding potential of -100 mV to 0 mV for 20 s (P1), to -100 mV for varying durations and then to 0 mV for 20 ms (P2) every 120 s. The peak amplitude of LTCC currents in P2 was normalized to that in P1, plotted against the duration between P1 and P2 and fit with the following equation:

$$r = 1 - A_f \, exp \, (-t / \tau_f) - A_s \, exp \, (-t / \tau_s) \quad \text{(Eq. 4)}$$

, where r is recovery; and t, duration at -100 mV. Figs. 3-5 and Table 1 show A_f, A_s, and A_0 values

normalized to the sum of these values.

To analyze isochronal inactivation, the membrane potential was depolarized from -80 mV to 0 mV for 50 ms (P1), repolarized to -80 mV for 5 ms, changed to potentials between -100 and 0 mV for 30 s with a 10 mV increment, repolarized to -80 mV for 5 ms, and then depolarized to 0 mV for 50 ms (P2) every 120 s. The peak LTCC current amplitude in P2 was normalized that in P1, plotted against membrane potentials and fit with the following equation:

$$f = 1 / (1 + exp ((E_m - E_{0.5\_Inact}) / k_{\_Inact})) \quad \text{(Eq. 5)}$$

, where f is availability; $E_{0.5\_Inact}$, half-maximum inactivation potential; and $k_{\_Inact}$, slope factor of inactivation.

Recorded membrane currents were low-pass filtered at 10 kHz (-3 dB), digitized at 47.2 kHz with a PCM converter system (VR-10B; Instrutech Corp., New York, NY) and recorded on videocassette tapes. For off-line analysis, data were reproduced, low-pass filtered at 2 kHz (-3 dB), digitized at 5 kHz with an AD converter (ITC16I; Instrutech Corp.) and analyzed with Patch Analyst Pro (MT Corp., Hyogo, Japan).

2.4 Statistical Analysis

Data are shown as the means ± S.E.M. Statistical significance was evaluated with Student's paired or unpaired *t*-test. For the multiple comparisons of data, analysis of variance with Bonferroni's test was used. $P < 0.05$ was considered significant.

3. Results

3.1 Current-voltage relationship of LTCC (WT) and LTCC (G436R) channels

First, the current-voltage relationship of LTCCS with and without the Timothy mutation (LTCC (G436R) and LTCC (WT), respectively) was analyzed with Ba^{2+} as a charge carrier. As shown in Fig. 1A, both peak LTCC (WT) and LTCC (G436R) currents progressively increased at potentials between -40 and 0 mV and then decreased at potentials between +10 and +50 mV, yielding almost identical, prototypical U-shaped peak current-voltage relationships (Fig. 1B). Lines are the fit of the averaged data with Eq. 1 with parameters summarized in Table 1. Each parameter was not significantly different between these channels. The decay of the currents reflects OSI. Although the OSI of LTCC (WT) channels was slow, LTCC (G436R) channels exhibited even slower OSI, especially at potentials more positive to 0 mV as previously reported (Barrett and Tsien, 2008; Raybaud et al., 2006; Splawski et al., 2005; Splawski et al., 2004; Yarotskyy et al., 2009).

3.2 Tonic block of LTCC (WT) and LTCC (G436R) channels by nifedipine at -80 mV

The tonic block of these channels by nifedipine was assessed at the holding potential of -80 mV (Fig. 2). Although LTCC (G436R) exhibited impaired VDI compared with LTCC (WT), nifedipine inhibited both channels in a similar concentration-dependent manner. The fit of the averaged data with Eq. 2 (lines) indicated that the $K_{0.5}$ of nifedipine was 10 and 11 nmol/L for LTCC (WT) and LTCC (G436R) channels, respectively. Thus, nifedipine exerted an almost equipotent tonic block of these channels at -80 mV.

3.3 Effect of nifedipine on LTCC (WT) and LTCC (G436R) channels at -40 mV

We next examined the effect of nifedipine at -40 mV where channels exhibit CSI. In the absence of nifedipine, both LTCC (WT) and LTCC (G436R) channels were inactivated in a time-dependent manner (Fig. 3A). Lines are the fit of the data with a biexponential function (Eq. 3). Both channels exhibited a similar fast time constant (τ_f), relative amplitude of a slow component (A_s) and relative amplitude of non-inactivating component (A_0) (Fig. 3B, Table 1). A slow time constant (τ_s) tended to

be larger in LTCC (G436R) than LTCC (WT) channels, but this difference did not reach statistical significance. The relative amplitude of a fast component (A_f) of LTCC (G436R) channels was significantly smaller than that of LTCC (WT) channels. Nifedipine (3 nmol/L), which inhibited both LTCC (WT) and LTCC (G436R) by ~40% (Fig. 2), significantly increased A_f to a comparable level in these channels. Nifedipine also significantly decreased τ_s in both channels. Consequently, nifedipine diminished the difference in CSI at -40 mV between the channels.

3.4 Effect of nifedipine on LTCC (WT) and LTCC (G436R) channels at 0 mV

Fig. 4 shows the effect of nifedipine on LTCC (WT) and LTCC (G436R) currents at 0 mV. To enable both channels to be fully inactivated within a voltage pulse, we applied a 20s voltage step to cells. In the absence of nifedipine, LTCC (G436R) currents exhibited slower OSI than LTCC (WT) currents (Fig. 4A). The fit of the current decay with a biexponential function (Eq. 3) indicates that both τ_f and τ_s were significantly larger in LTCC (G436R) than LTCC (WT) channels (Fig. 4B, Table 1). In addition, A_f was significantly smaller and A_s was significantly larger in LTCC (G436R) than LTCC (WT) channels. A_0 was small and not significantly different between the channels. Nifedipine (3 nmol/L) accelerated OSI of both currents. Nifedipine significantly decreased τ_f without affecting other parameters in LTCC (WT) channels. On the other hand, nifedipine did not significantly affect τ_f or τ_s but significantly increased A_f and decreased A_s in LTCC (G436R) channels. Thus, nifedipine caused a shift of the relative population of the fast and slow components in LTCC (G436R) channels. As a result, the decay of LTCC (G436R) currents in the presence of nifedipine was similar to that of LTCC (WT) currents in the absence of nifedipine.

3.5 Effect of nifedipine on the recovery from inactivation of LTCC (WT) and LTCC (G436R) channels at -100 mV

Fig. 5A shows the time course of the recovery from the OSI of LTCC (WT) and LTCC (G436R) channels at -100 mV in the presence and absence of 3 nmol/L nifedipine. Almost complete OSI was induced by a conditional prepulse to 0 mV for 20s. Lines are the fit of the averaged data with a

biexponential function (Eq. 4). In the absence of nifedipine, LTCC (G436R) channels recovered from OSI much more slowly than LTCC (WT) channels. Compared with LTCC (WT) channels, LTCC (G436R) channels possessed similar τ_f and τ_s but significantly smaller A_f and larger A_s (Fig. 5B, Table 1). Interestingly, nifedipine decelerated the recovery of LTCC (WT) channels whereas it accelerated that of LTCC (G436R) channels (Fig. 5A). Kinetic analysis indicated that nifedipine significantly increased τ_s but not τ_f in both channels (Fig. 5B, Table 1). Although nifedipine did not affect the other parameters in LTCC (WT) channels, it significantly increased A_f and decreased A_s in LTCC (G436R) channels. As a result, nifedipine diminished the difference in the recovery from VDI between the channels.

3.6 Effect of nifedipine on the isochronal inactivation of LTCC (WT) and LTCC (G436R) channels

We finally examined the effect of nifedipine on the isochronal inactivation of LTCC (WT) and LTCC (G436R) channels in conditional pulses to different membrane potentials (Fig. 6). Lines are the fit of the averaged data with a Boltzmann function (Eq. 5). Neither the half-maximum inactivation potential nor a slope factor was significantly different between LTCC (WT) and LTCC (G436R) channels in the absence of nifedipine (Table 1). Nifedipine significantly caused a leftward shift of the inactivation curve by ~7 mV in LTCC (WT) channels and by ~11 mV in LTCC (G436R) channels.

4. Discussion

4.1 Model of $Ca_V1.2$ L-type Ca^{2+} channels

Both LTCC (WT) and LTCC (G436R) exhibited biexponential CSI (Fig. 3), OSI (Fig. 4) and recovery from OSI (Fig. 5), indicating that they may have fast and slow VDI sates. Fig. 7A illustrates the minimum state diagram of LTCCs. C_0 is a closed state occurring at deeply hyperpolarized potentials whereas C_4 is a pre-open closed state prevailing at the sub-threshold potential (Yarotskyy et al., 2009). Upon depolarization from hyperpolarized potentials to supra-threshold potentials, LTCCs transit from C_0 to C_4 and then to an open state (O). Each closed and open state is connected with fast inactivated states (I_{cf0}---I_{cf4}, I_{of}) and slow inactivated states (I_{cs0}---I_{cs4}, I_{os}). Nifedipine independently binds to each state (asterisks).

4.2 Comparison of LTCC (WT) and LTCC (G436R) channels in the absence of nifedipine

LTCC (WT) and LTCC (G436R) were activated at potentials positive to -30 mV and exhibited an almost identical current-voltage-relationship (Fig. 1), indicating that activation (C_0---O) is similar in these channels. It was reported that LTCC (G436R) channels exhibited slower activation and deactivation than LTCC (WT) channels (Yarotskyy et al., 2009); however, the steady-state activation does not seem to be significantly different between these channels.

At -40 mV, most LTCCs may transit from C_4 to I_{cf4} and I_{cs4} (Fig. 7A). LTCC (G436R) exhibited smaller A_f than LTCC (WT) (Fig. 3), indicating that the mutation selectively impairs I_{cf4} and thus, that $L_{I\text{-}II}$ supports I_{cf4}. Yarotskyy et al. reported that the G436R mutation did not affect CSI at -60 mV (Yarotskyy et al., 2009). Thus, $L_{I\text{-}II}$ seems to support fast CSI at potentials positive to the sub-threshold potential. At 0 mV, LTCCs exhibited OSI (O-I_{of}, O-I_{os}) (Fig. 7A). We found stronger OSI of LTCC (G436R) than previously reported (Fig. 4) (Barrett and Tsien, 2008; Raybaud et al., 2006; Splawski et al., 2004; Yarotskyy et al., 2009), probably due to the higher intracellular free Mg^{2+} concentration used in this than previous studies (Brunet et al., 2009). The twice larger A_f than A_s of LTCC (WT) indicates that the O-I_{of} transition predominates over the O-I_{os} transition. Although LTCC (G436R) exhibited significantly larger τ_f and τ_s than LTCC (WT), it showed significantly

smaller A_f and larger A_s. Thus, the mutation may more severely impair I_{of} than I_{os} so that I_{os} compensated for the impaired I_{of}. Thus, $L_{I\text{-}II}$ may mainly support I_{of}, and the increased τ_s of LTCC (G436R) may be secondary to the impaired I_{of}. At a voltage step to -100 mV from 0 mV, both channels exhibited biexponential recovery from OSI (Fig. 5), indicating the coexistence of the recovery from I_{of} and I_{os}. Here, we assume that the recovery from I_{of} is faster than that from I_{os} because the recovery was faster after a shorter conditioning pulse in both channels (data not shown). Neither τ_f nor τ_s was significantly different between LTCC (WT) and LTCC (G436R), indicating the similarity in the kinetics of these channels at -100 mV; however, LTCC (G436R) exhibited significantly smaller A_f and larger A_s than LTCC (WT), which probably reflects the difference in A_f and A_s of OSI in the preceding conditional pulse between the channels (Fig. 3).

Fig. 7B schematically illustrates different states of $Ca_V1.2$ subunits. Because the G436R mutation mainly impaired fast CSI and OSI, fast inactivated states are illustrated to arise from the docking of $L_{I\text{-}II}$ to S6 (Fig. 7B) (Stotz et al., 2000; Stotz and Zamponi, 2001). Because slow OSI and CSI were not affected by the mutation, they are shown to be caused by other mechanisms such as the conformational change of VSD, depletion of Ca^{2+} ions in the selectivity filter and/or the conformational change of the cytoplasmic end of S6 (Hadley and Lederer, 1991; Peterson and Catterall, 2006; Shi and Soldatov, 2002; Shirokov et al., 1992). Note that nifedipine bound to $Ca_V1.2$ subunits is also depicted and that different shapes of the DHP receptor represent its state-dependent change in the affinity for nifedipine.

4.3 Comparison of the effects of nifedipine on LTCC (WT) and LTCC (G436R) channels

Nifedipine modified the kinetics of LTCC (WT) and LTCC (G436R) upon depolarization (Figs. 3 and 4) and repolarization (Fig. 5). These effects of nifedipine would reflect a voltage-dependent change in the interaction between LTCC and nifedipine. At -40 mV, nifedipine increased A_f in both channels as reported for other DHPs (Berjukow and Hering, 2001; Berjukow et al., 2000) and abolished the difference in A_f between the channels (Fig. 3), indicating that I_{cf4} has higher affinity for nifedipine than C_4 (Fig. 7B). It is probable that nifedipine allosterically interacts with $L_{I\text{-}II}$ which

docks to IIIS6 harboring the DHP receptor (Stotz et al., 2000) and thereby augments fast CSI. Nifedipine also decreased τ_s in both channels. It is difficult to interpret this phenomenon if we assume that C_4* does not become conductive when converted to O*. If this were the case, CSI would reflect only a time-dependent decrease in C4, and nifedipine must accelerate this process. However, the nifedipine-induced I_{cs4}-I_{cs4}* transition cannot accelerate the C_4-I_{cs4}-I_{cs4}* transition. Thus, we propose that O* is conductive and that the C_4*-I_{cs4}* transition is faster than the C_4-I_{cs4} transition (Fig. 7B).

At 0 mV, nifedipine decreased τ_f in LTCC (WT) (Fig. 4). The acceleration of the decay of LTCC Ba^{2+} currents by DHP antagonists arise from the open-channel block (Handrock et al., 1999; Lacinova et al., 2000; Lee and Tsien, 1983; Sanguinetti and Kass, 1984), drug-induced inactivation (Berjukow and Hering, 2001; Berjukow et al., 2000) or acceleration of intrinsic VDI (Hess et al., 1984), but no consensus has been reached. Because we consider that O* is conducting, we reject the possibility of the open-channel block and propose that the O*-I_{of}* transition is faster than the O-I_{of} transition due to the promoted docking of $L_{I\text{-}II}$ to S6. Thus, I_{of} may have higher affinity for nifedipine than O (Fig. 7B). On the other hand, nifedipine did not affect τ_s or A_s in LTCC (WT), suggesting that O and I_{os} have similar affinity for nifedipine (Fig. 7B). In LTCC (G436R), nifedipine did not significantly affect τ_f or τ_s but significantly increased A_f and decreased A_s. Thus, nifedipine might be unable to accelerate the docking of $L_{I\text{-}II}$ carrying the mutation to S6 but still capable of recruiting channels from the over-accumulated I_{os} into I_{of}* in LTCC (G436R).

In the recovery at -100 mV, nifedipine did not affect τ_f in either of the channels (Fig. 5), indicating that I_{cf0} does not have high affinity for nifedipine and thus, is not stabilized by the drug (Fig. 7B). On the other hand, nifedipine significantly increased τ_s in both channels, suggesting that I_{cs0} has higher affinity for nifedipine than C_0 (Fig. 7B). Other DHPs also selectively decelerated the slow component of recovery (Berjukow and Hering, 2001; Berjukow et al., 2000; Lacinova et al., 2000; Sanguinetti and Kass, 1984). Similar τ_f and τ_s of LTCC (WT) and LTCC (G436R) indicate that their kinetics were similar at -100 mV also in the presence of nifedipine. Although nifedipine did not affect A_f or A_s in LTCC (WT), it significantly increased A_f and decreased A_s in LTCC (G436R). This

may once again reflect the effect of nifedipine on A_f and A_s of OSI in the conditional pulse (Fig. 3). Thus, a kinetic difference between these channels at a deeply hyperpolarized potential is rather minor, which accounts for the insignificant difference in the tonic block of these channels by nifedipine at -80 mV (Fig. 2).

Taken together, nifedipine promoted fast CSI/OSI at potentials positive to the sub-threshold potential whereas it promoted and stabilized slow CSI at potentials negative to the sub-threshold potential. Hering and his colleagues reported that DHP antagonists (+)- and (-)-isradipine caused an enantioselective tonic block at hyperpolarized potentials but equipotently accelerated the decay of LTCCs at depolarized potentials (Handrock et al., 1999). They found that the former but not the latter effect was disrupted by the mutation of the DHP-binding site in IVS6. Lacinova et al. showed that the same mutation selectively abolished slow but not fast recovery from VDI in the presence of isradipine (Lacinova et al., 2000). These reports together with the present results suggest that DHP might interact mainly with IIIS5/S6 at depolarized potentials, allosterically modulating the docking of L_{I-II} to IIIS6 and thereby promoting intrinsic fast VDI. On the other hand, DHP might interact mainly with IVS6 at hyperpolarized potentials and allosterically modulate slow VDI.

5 Conclusion

Nifedipine has two mechanistically distinct effects on LTCCs: the promotion of fast CSI/OSI caused by L_{I-II} at potentials positive to the sub-threshold potential and the promotion or stabilization of slow CSI at potentials negative to the sub-threshold potential. These two different mechanisms may underlie the phasic and tonic block of LTCCs by DHP, respectively.

Nifedipine normalized VDI kinetics of LTCCs with the Timothy syndrome mutation. Yarotskyy et al. also reported that roscovitine accelerates OSI of LTCC (G436R) (Yarotskyy et al., 2009). Thus, these agents may effectively ameliorate the complex excitotoxicity of the Timothy mutation and the resultant developmental and physiological abnormalities in patients with Timothy syndrome.

Acknowledgement

We are grateful to Ms. Reiko Sakai for secretarial assistance.

References

Barrett, C.F., Tsien, R.W., 2008. The Timothy syndrome mutation differentially affects voltage- and calcium-dependent inactivation of CaV1.2 L-type calcium channels. Proc Natl Acad Sci U S A 105, 2157-2162.

Bean, B.P., 1984. Nitrendipine block of cardiac calcium channels: high-affinity binding to the inactivated state. Proc Natl Acad Sci U S A 81, 6388-6392.

Berjukow, S., Hering, S., 2001. Voltage-dependent acceleration of Ca(v)1.2 channel current decay by (+)- and (-)-isradipine. Br J Pharmacol 133, 959-966.

Berjukow, S., Marksteiner, R., Gapp, F., Sinnegger, M.J., Hering, S., 2000. Molecular mechanism of calcium channel block by isradipine. Role of a drug-induced inactivated channel conformation. J Biol Chem 275, 22114-22120.

Brunet, S., Scheuer, T., Catterall, W.A., 2009. Cooperative regulation of Ca(v)1.2 channels by intracellular Mg(2+), the proximal C-terminal EF-hand, and the distal C-terminal domain. J Gen Physiol 134, 81-94.

Catterall, W.A., 2000. Structure and regulation of voltage-gated Ca2+ channels. Annu Rev Cell Dev Biol 16, 521-555.

Hadley, R.W., Lederer, W.J., 1991. Properties of L-type calcium channel gating current in isolated guinea pig ventricular myocytes. J Gen Physiol 98, 265-285.

Handrock, R., Rao-Schymanski, R., Klugbauer, N., Hofmann, F., Herzig, S., 1999. Dihydropyridine enantiomers block recombinant L-type Ca2+ channels by two different mechanisms. J Physiol 521 Pt 1, 31-42.

Hering, S., Berjukow, S., Sokolov, S., Marksteiner, R., Weiss, R.G., Kraus, R., Timin, E.N., 2000. Molecular determinants of inactivation in voltage-gated Ca2+ channels. J Physiol 528 Pt 2, 237-249.

Herlitze, S., Hockerman, G.H., Scheuer, T., Catterall, W.A., 1997. Molecular determinants of inactivation and G protein modulation in the intracellular loop connecting domains I and II of the calcium channel alpha1A subunit. Proc Natl Acad Sci U S A 94, 1512-1516.

Hess, P., Lansman, J.B., Tsien, R.W., 1984. Different modes of Ca channel gating behaviour favoured by dihydropyridine Ca agonists and antagonists. Nature 311, 538-544.

Hockerman, G.H., Peterson, B.Z., Johnson, B.D., Catterall, W.A., 1997. Molecular determinants of drug binding and action on L-type calcium channels. Annu Rev Pharmacol Toxicol 37, 361-396.

Kammann, M., Laufs, J., Schell, J., Gronenborn, B., 1989. Rapid insertional mutagenesis of DNA by polymerase chain reaction (PCR). Nucleic Acids Res 17, 5404.

Kobrinsky, E., Kepplinger, K.J., Yu, A., Harry, J.B., Kahr, H., Romanin, C., Abernethy, D.R., Soldatov, N.M., 2004. Voltage-gated rearrangements associated with differential beta-subunit modulation of the L-type Ca(2+) channel inactivation. Biophys J 87, 844-857.

Lacinova, L., Klugbauer, N., Hofmann, F., 2000. State- and isoform-dependent interaction of isradipine with the alpha1C L-type calcium channel. Pflugers Arch 440, 50-60.

Lee, K.S., Tsien, R.W., 1983. Mechanism of calcium channel blockade by verapamil, D600, diltiazem and nitrendipine in single dialysed heart cells. Nature 302, 790-794.

Peterson, B.Z., Catterall, W.A., 2006. Allosteric interactions required for high-affinity binding of dihydropyridine antagonists to Ca(V)1.1 Channels are modulated by calcium in the pore. Mol Pharmacol 70, 667-675.

Raybaud, A., Dodier, Y., Bissonnette, P., Simoes, M., Bichet, D.G., Sauve, R., Parent, L., 2006. The role of the GX9GX3G motif in the gating of high voltage-activated Ca2+ channels. J Biol Chem 281, 39424-39436.

Sanguinetti, M.C., Kass, R.S., 1984. Voltage-dependent block of calcium channel current in the calf cardiac Purkinje fiber by dihydropyridine calcium channel antagonists. Circ Res 55, 336-348.

Shi, C., Soldatov, N.M., 2002. Molecular determinants of voltage-dependent slow inactivation of the Ca2+ channel. J Biol Chem 277, 6813-6821.

Shirokov, R., Levis, R., Shirokova, N., Rios, E., 1992. Two classes of gating current from L-type Ca channels in guinea pig ventricular myocytes. J Gen Physiol 99, 863-895.

Soldatov, N.M., 2003. Ca2+ channel moving tail: link between Ca2+-induced inactivation and Ca2+ signal transduction. Trends Pharmacol Sci 24, 167-171.

Splawski, I., Timothy, K.W., Decher, N., Kumar, P., Sachse, F.B., Beggs, A.H., Sanguinetti, M.C., Keating, M.T., 2005. Severe arrhythmia disorder caused by cardiac L-type calcium channel mutations. Proc Natl Acad Sci U S A 102, 8089-8096; discussion 8086-8088.

Splawski, I., Timothy, K.W., Sharpe, L.M., Decher, N., Kumar, P., Bloise, R., Napolitano, C., Schwartz, P.J., Joseph, R.M., Condouris, K., Tager-Flusberg, H., Priori, S.G., Sanguinetti, M.C., Keating, M.T., 2004. Ca(V)1.2 calcium channel dysfunction causes a multisystem disorder including arrhythmia and autism. Cell 119, 19-31.

Stotz, S.C., Hamid, J., Spaetgens, R.L., Jarvis, S.E., Zamponi, G.W., 2000. Fast inactivation of voltage-dependent calcium channels. A hinged-lid mechanism? J Biol Chem 275, 24575-24582.

Stotz, S.C., Jarvis, S.E., Zamponi, G.W., 2004. Functional roles of cytoplasmic loops and pore lining transmembrane helices in the voltage-dependent inactivation of HVA calcium channels. J Physiol 554, 263-273.

Stotz, S.C., Zamponi, G.W., 2001. Structural determinants of fast inactivation of high voltage-activated Ca(2+) channels. Trends Neurosci 24, 176-181.

Yamada, M., Ohta, K., Niwa, A., Tsujino, N., Nakada, T., Hirose, M., 2008. Contribution of L-type Ca2+ channels to early afterdepolarizations induced by I Kr and I Ks channel suppression in guinea pig ventricular myocytes. J Membr Biol 222, 151-166.

Yarotskyy, V., Gao, G., Peterson, B.Z., Elmslie, K.S., 2009. The Timothy syndrome mutation of cardiac CaV1.2 (L-type) channels: multiple altered gating mechanisms and pharmacological restoration of inactivation. J Physiol 587, 551-565.

Zuhlke, R.D., Pitt, G.S., Deisseroth, K., Tsien, R.W., Reuter, H., 1999. Calmodulin supports both inactivation and facilitation of L-type calcium channels. Nature 399, 159-162.

Figure legends

Fig. 1. Current-voltage relationship of L-type Ca^{2+} channels with or without G436R mutation. (A) Top panel: voltage protocol. Middle and bottom panels: representative whole-cell Ba^{2+} currents of wild-type L-type Ca^{2+} channels (LTCC (WT)) and LTCCs with the G436R mutation (LTCC (G436R)) in response to depolarization to potentials between -40 and 0 mV (middle panels) and those between +10 and +50 mV (bottom panels) with a 10 mV increment. (B) Peak current-voltage relationships of LTCC (WT) and LTCC (G436R) channels. The peak current amplitude in different voltage steps was normalized to the maximum peak current amplitude in each cell. Symbols and bars indicate the mean ± S.E.M. Lines are the fit of the data with Eq. 1. The parameters obtained with fitting are summarized in Table 1.

Fig. 2. Concentration-dependent tonic block by nifedipine of LTCC (WT) and LTCC (G436R) currents. Top panel: voltage protocol. Bottom panel: concentration-dependent effect of nifedipine. Nifedipine was cumulatively applied to cells. The peak LTCC current amplitude at 0 mV in the presence of each concentration of nifedipine was normalized to that in the presence of 0.1% DMSO and plotted against the concentration of nifedipine. Symbols and bars indicate the mean ± S.E.M. Lines are the fit of the data with Eq. 2.

Fig. 3. Effect of nifedipine on inactivation of LTCC (WT) and LTCC (G436R) channels at -40 mV. (A) Top panel: voltage protocol. Bottom panels: a time-dependent decrease in the availability of LTCC (WT) and LTCC (G436R) channels at -40 mV in the absence (CONT) and presence (NIF) of 3 nmol/L nifedipine. Peak LTCC current amplitude in P2 was normalized to that in P1 and plotted against the duration at -40 mV. Symbols and bars indicate the mean ± S.E.M. Lines are the fit of the data with Eq. 3. (B) Parameters used to fit the decay of availability of LTCC (WT) and LTCC (G436R) channels at -40 mV with Eq. 3 (Table 1). Data are shown as the means ± S.E.M. *: $P < 0.05$ vs. CONT; **: $P < 0.01$ vs. CONT; ††: $P < 0.01$ vs. WT.

Fig. 4. Effect of nifedipine on inactivation of LTCC (WT) and LTCC (G436R) channels at 0 mV. (A) Top panel: voltage protocol. Bottom panels: representative whole-cell currents of LTCC (WT) and LTCC (G436R) channels at 0 mV in the absence and presence of 3 nmol/L nifedipine. LTCC currents are normalized to the peak current amplitude. (B) Parameters used to fit the decay of whole-cell LTCC (WT) and LTCC (G436R) currents with Eq. 3 (Table 1). Data are shown as the means ± S.E.M. *: $P < 0.05$ vs. CONT; †: $P < 0.05$ vs. WT; †††: $P < 0.001$ vs. WT.

Fig. 5. Effect of nifedipine on recovery of LTCC (WT) and LTCC (G436R) channels at -100 mV. (A) Top panel: voltage protocol. Bottom panels: the recovery from inactivation of LTCC (WT) and LTCC (G436R) channels at -100 mV in the absence and presence of 3 nmol/L nifedipine. Peak amplitude of LTCC currents in P2 was normalized to that in P1, and plotted against the duration between P1 and P2. Symbols and bars indicate the mean ± S.E.M. Lines are the fit of the data with Eq. 4. (B) Parameters used to fit Eq. 4 to the time course of the recovery from inactivation of LTCC (WT) and LTCC (G436R) channels in the presence and absence of nifedipine (Table 1). Data are shown as the means ± S.E.M. *: $P < 0.05$ vs. CONT; ***: $P < 0.001$ vs. CONT; †: $P < 0.05$ vs. WT.

Fig. 6. Effect of nifedipine on isochronal inactivation of LTCC (WT) and LTCC (G436R) channels. Top panel: voltage protocol. Middle and bottom panels: isochronal inactivation of LTCC (WT) and LTCC (G436R) in the absence and presence of 3 nmol/L nifedipine. Peak LTCC current amplitude in P2 was normalized to that in P1 (*f*) and plotted against membrane potentials. Symbols and bars indicate the mean ± S.E.M. Lines are the fit of the data with Eq. 5 with parameters summarized in Table 1.

Fig. 7. Allosteric model of L-type Ca^{2+} channels. (A) State diagram of LTCCS. C: closed state; O: open state; I_{cf}: closed fast-inactivated state; I_{cs}: closed slow-inactivated state; I_{of}: open fast-inactivated state; I_{os}: open slow-inactivated state. Asterisks indicate nifedipine-bound states. All interconversions are in principle voltage-dependent. The equilibria and rates for interconversion

between nifedipine-free states and between nifedipine-bound states are different. (B) Schematic representation of the side view of LTCCS in the presence and absence of nifedipine. The plasma membrane is depicted as gray squares with the extracellular side upward. Schematics of inner helices formed from I-IVS6, the high-affinity DHP-binding site in III/IVS6, nifedipine, a selectivity filter, Ca^{2+} ions in the selectivity filter, $L_{I\text{-}II}$, G436 and voltage-sensing domains (VSDs) including S4 are shown. The circular DHP-binding site has higher affinity for nifedipine than the square site. Note that the upward movement of VSDs indicates the activation of LTCCs. Fast VDI is shown to be supported by $L_{I\text{-}II}$ that occludes the inner mouth of a channel pore by docking to S6. Slow VDI is shown to be associated with gating charge immobilization (indicated by tilted S4), depletion of Ca^{2+} ions in a selectivity filter (indicated by a single Ca^{2+} ion in a filter) and the conformational change of the cytoplasmic part of S6 (indicated by wavy lines). Three Ca^{2+} ions in the selectivity filter indicate conducting states whereas one Ca^{2+} ion in the filter represents non-conducting states.

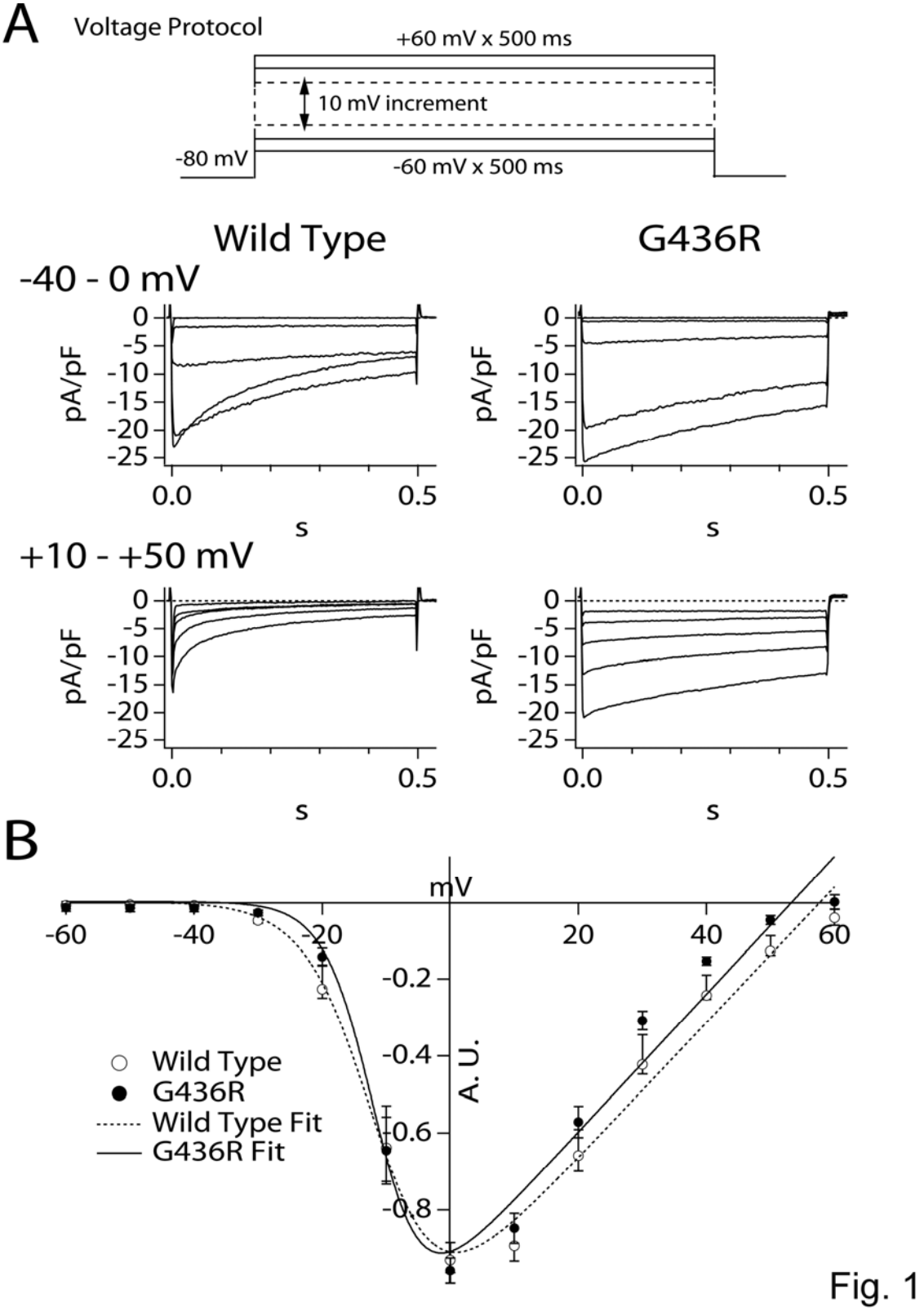
A
Voltage Protocol
+60 mV x 500 ms
10 mV increment
-80 mV
-60 mV x 500 ms
Wild Type
G436R
-40 - 0 mV
+10 - +50 mV
pA/pF
0
-5
-10
-15
-20
-25
0.0
0.5
s
B
mV
-60
-40
-20
20
40
60
-0.2
-0.4
-0.6
-0.8
A. U.
Wild Type
G436R
Wild Type Fit
G436R Fit

Fig. 1

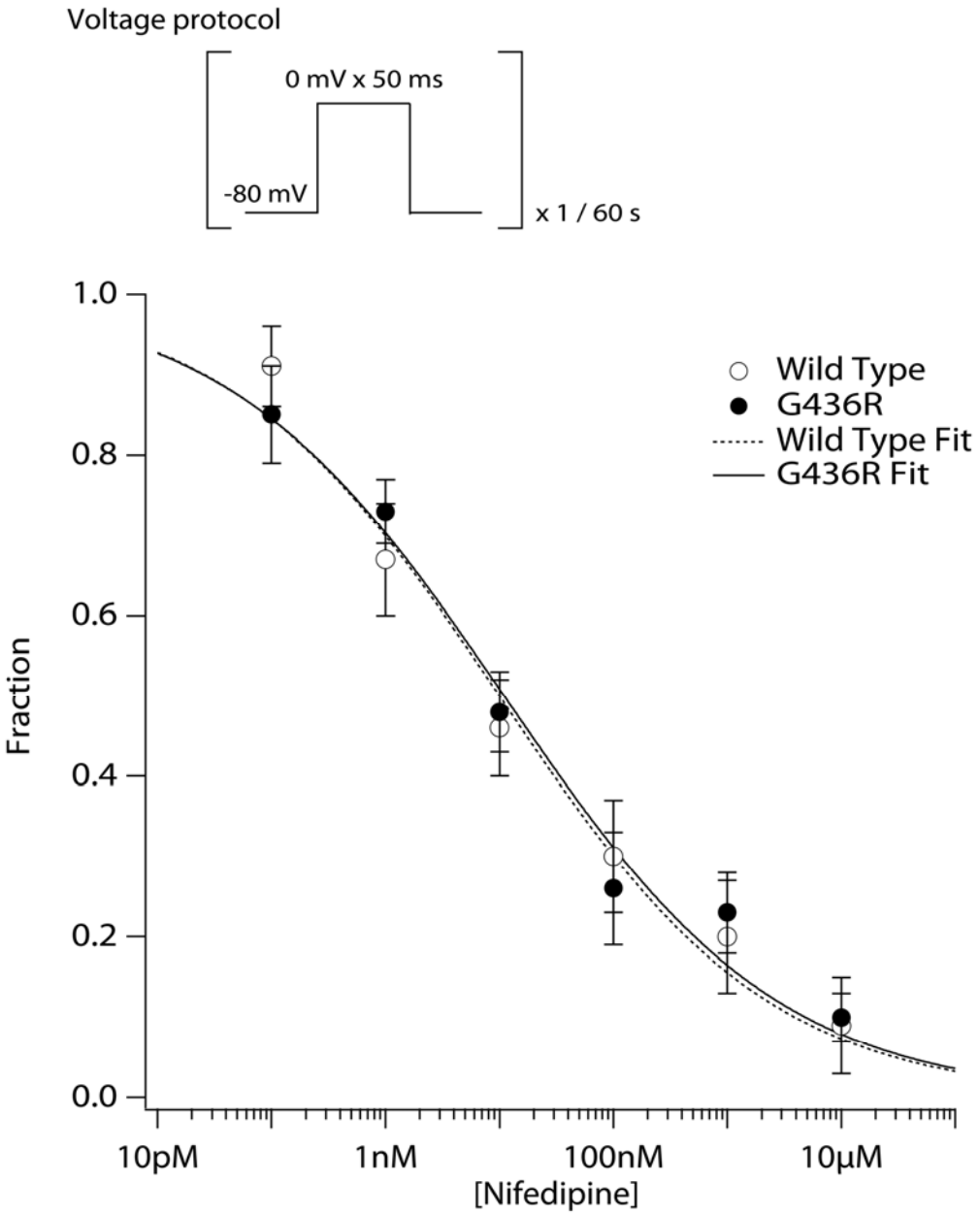
Voltage protocol
0 mV x 50 ms
-80 mV
x 1 / 60 s
1.0
0.8
0.6
0.4
0.2
0.0
Fraction
Wild Type
G436R
Wild Type Fit
G436R Fit
10pM
1nM
100nM
10µM
[Nifedipine]

Fig. 2

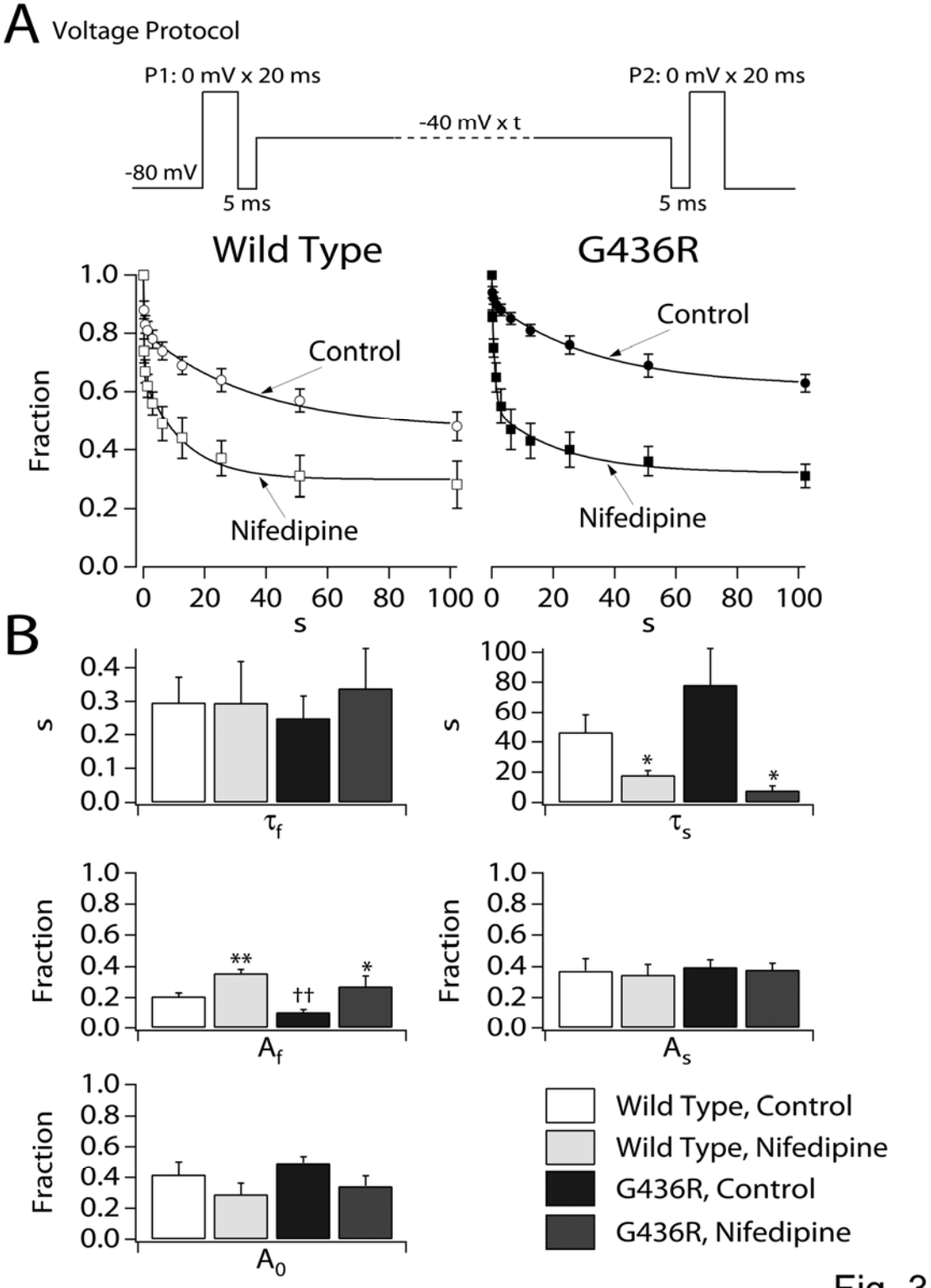
A
Voltage Protocol
P1: 0 mV x 20 ms
P2: 0 mV x 20 ms
-40 mV x t
-80 mV
5 ms
5 ms
Wild Type
G436R
Control
Nifedipine
Control
Nifedipine
Fraction
s
B
s
s
τ_f
τ_s
Fraction
Fraction
A_f
A_s
Fraction
A_0
Wild Type, Control
Wild Type, Nifedipine
G436R, Control
G436R, Nifedipine

Fig. 3

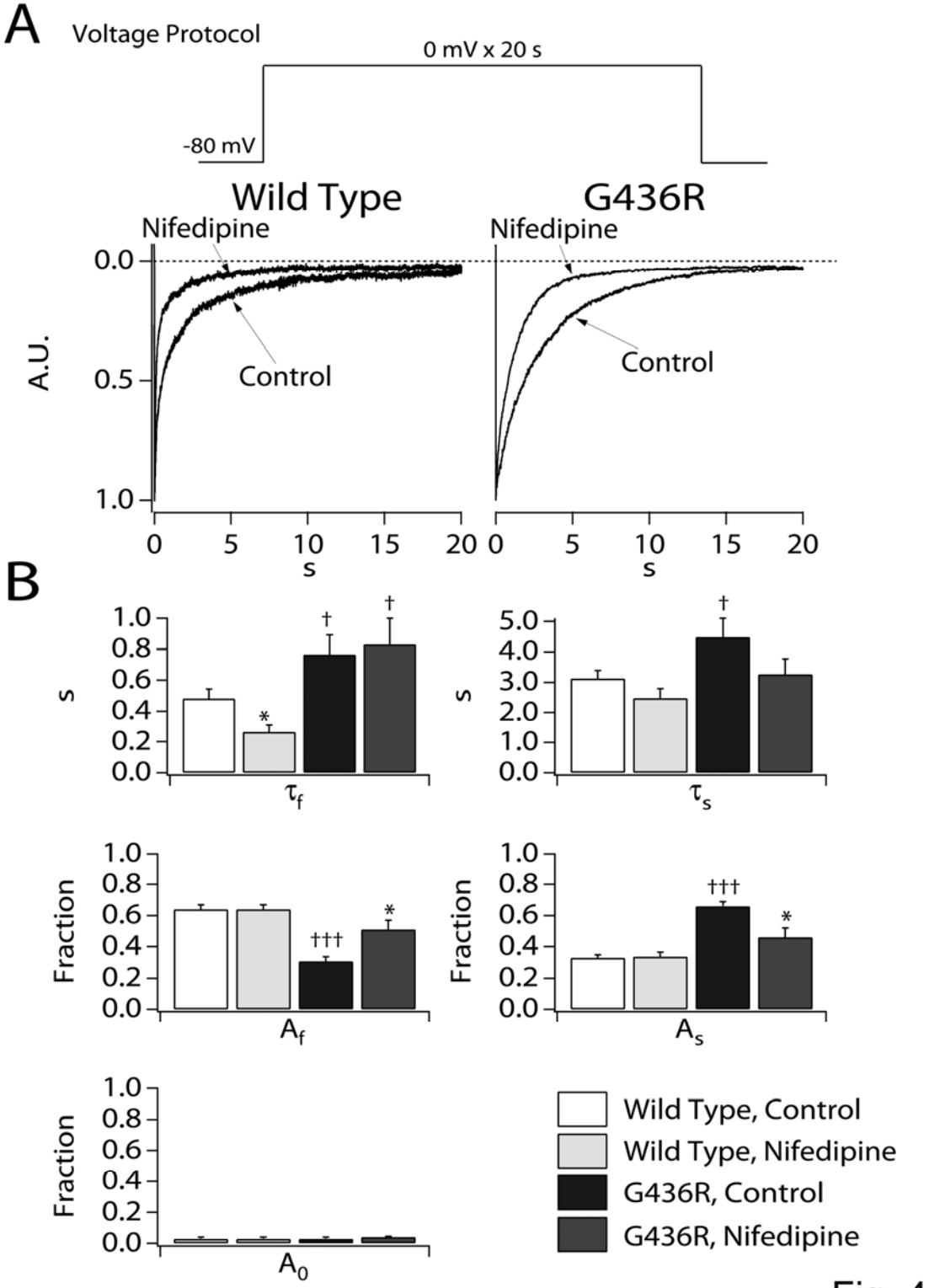
A
Voltage Protocol
0 mV x 20 s
-80 mV
Wild Type
G436R
Nifedipine
Nifedipine
Control
Control
A.U.
0.0
0.5
1.0
0
5
10
15
20
s
B
s
Fraction
τ_f
τ_s
A_f
A_s
A_0
Wild Type, Control
Wild Type, Nifedipine
G436R, Control
G436R, Nifedipine

Fig. 4

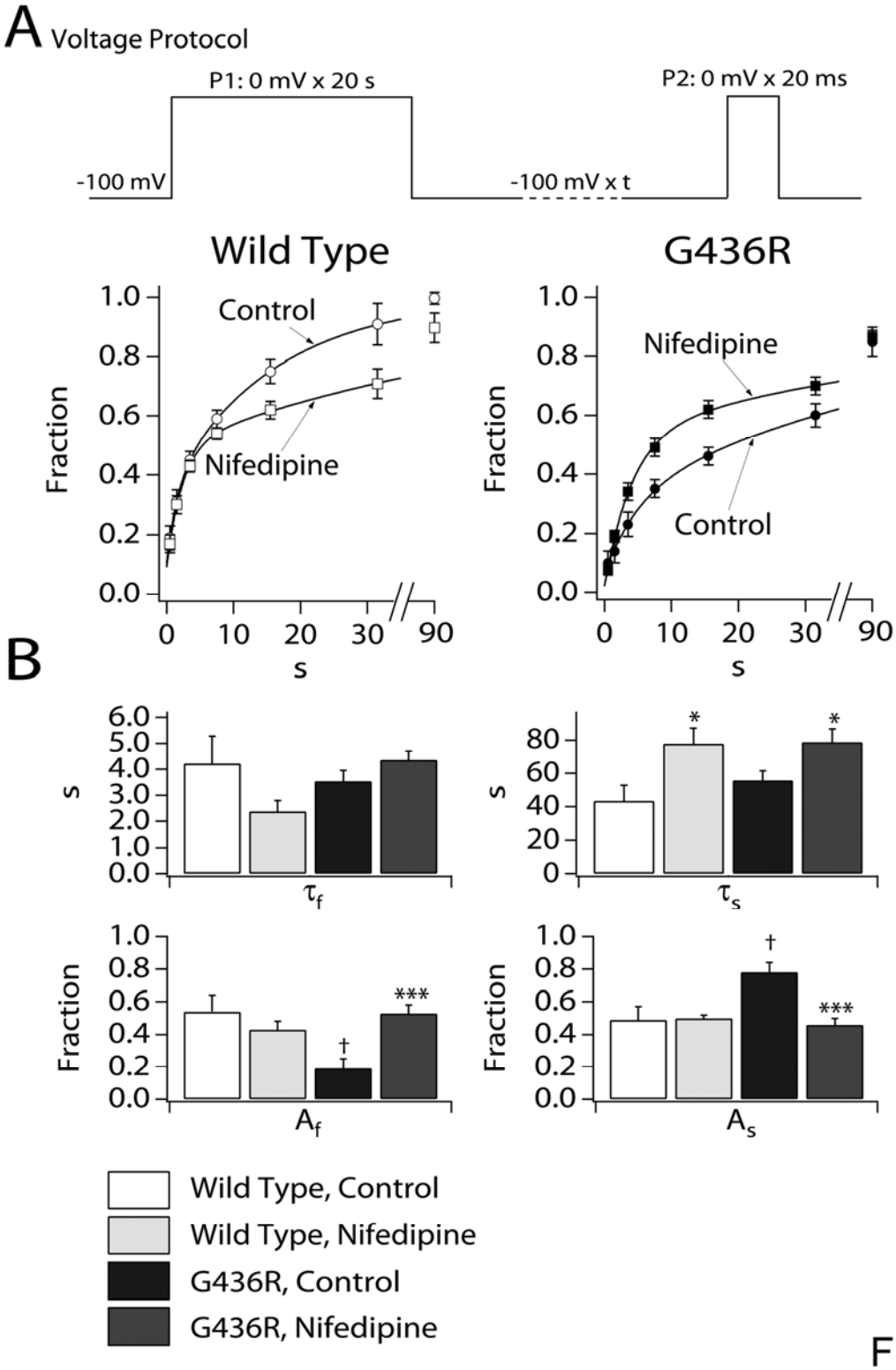
A
Voltage Protocol
P1: 0 mV x 20 s
P2: 0 mV x 20 ms
-100 mV
-100 mV x t
Wild Type
G436R
Control
Nifedipine
Fraction
s
B
τ_f
τ_s
A_f
A_s
Wild Type, Control
Wild Type, Nifedipine
G436R, Control
G436R, Nifedipine

Fig. 5

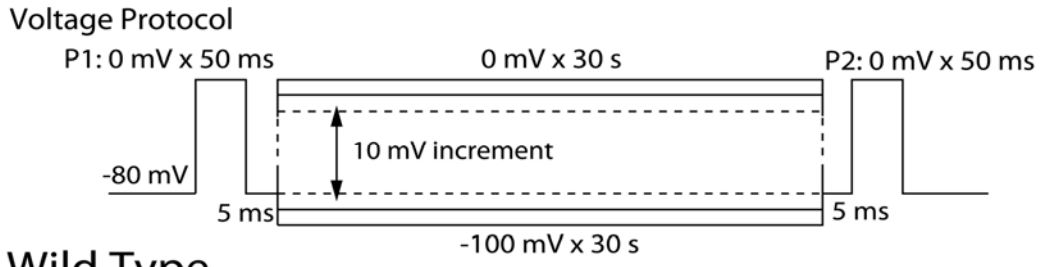

Wild Type

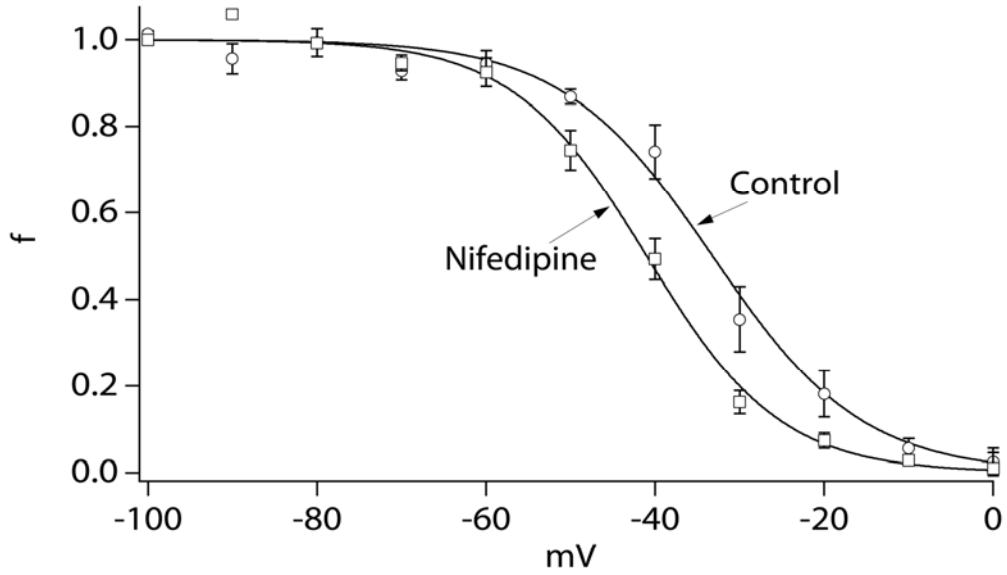

G436R

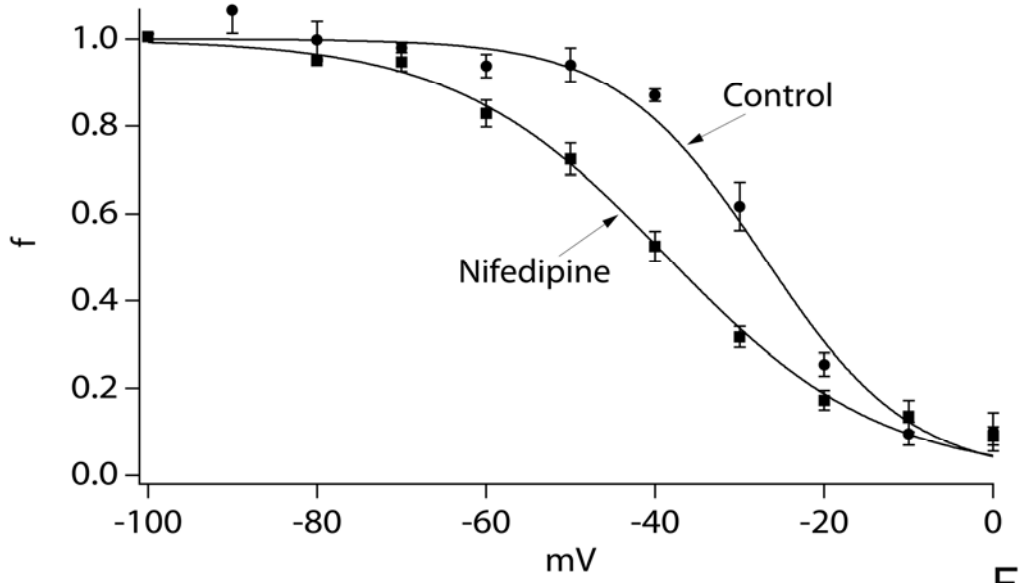

Fig. 6

Fig. 7

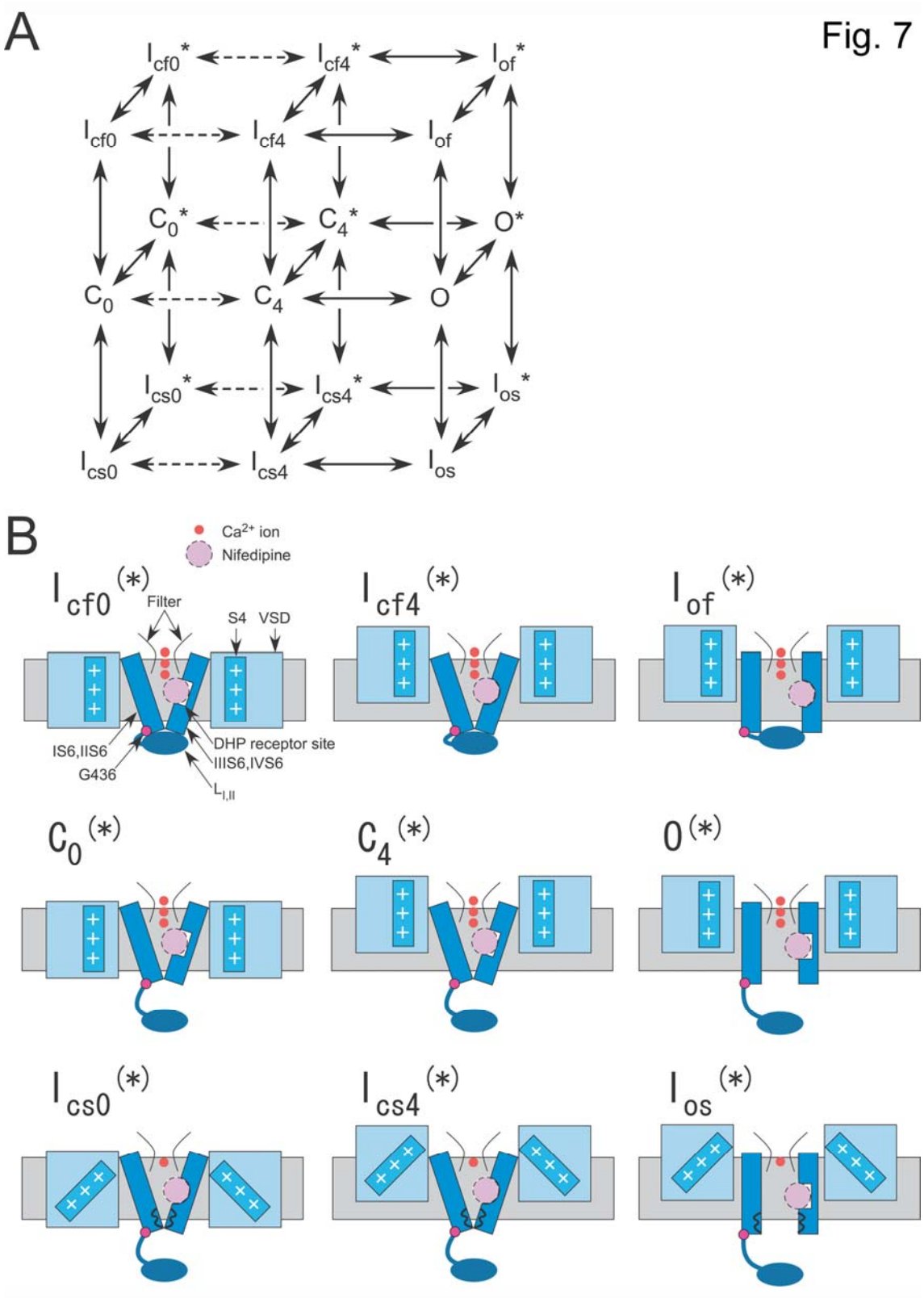
A
I_{cf0}^*
I_{cf4}^*
I_{of}^*
I_{cf0}
I_{cf4}
I_{of}
C_0^*
C_4^*
O^*
C_0
C_4
O
I_{cs0}^*
I_{cs4}^*
I_{os}^*
I_{cs0}
I_{cs4}
I_{os}
B
Ca^{2+} ion
Nifedipine
I_{cf0} (*)
Filter
S4
VSD
IS6,IIS6
G436
DHP receptor site
IIIS6,IVS6
$L_{I,II}$
I_{cf4} (*)
I_{of} (*)
C_0 (*)
C_4 (*)
O (*)
I_{cs0} (*)
I_{cs4} (*)
I_{os} (*)

Fig. S1

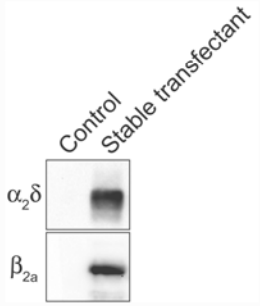

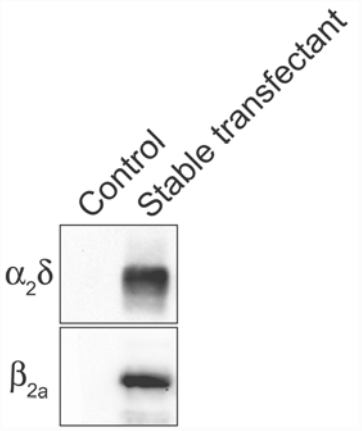
Control
Stable transfectant
$\alpha_2\delta$
β_{2a}